MODELLING PRESSURE-TRANSPORT FOR TURBULENT WAKE FLOWS

Kazuhiko Suga
Toyota Central Research and Development Laboratories, Inc.
Nagakute, Aichi, 480-1192, Japan
k-suga@mosk.tytlabs.co.jp

ABSTRACT

Modelling the pressure-transport term of the Reynolds stress transport equation is presented focusing on the third rank tensor of the rapid part of the pressure-velocity correlation. The proposed model term is added to a low Reynolds number two-component-limit full second moment closure and its effects are discussed through applications for turbulent wake and separating flows.

INTRODUCTION

In any standard or advanced RANS turbulence closure, it has rarely been considered to be important to model the pressure-transport separately from the other processes. Some exceptional models attempted to include effects of the pressure-transport near a wall since the DNSs of turbulent wall shear flows (Mansour *et al.*, 1988, Spalart, 1988, *etc.*) indicated that it was only important in the region very near a wall to partly balance with the dissipation rate. Amongst those, Kawamura and Kawashima (1994) and Nagano and Shimada (1995) employed a term including the second derivative of the dissipation rate to take account of this effect in the turbulence energy equation. The theoretical background of using such a term came from the proposal of Yoshizawa (1987) by the two-scale direct-interaction approximation (TSDIA).

Recently, the DNS by Yao *et al.*(2001) pointed out that the effects of the pressure-transport process were significant in the recirculating flow region of a turbulent wake flow behind a rectangular trailing-edge. In fact, its magnitude was comparable to that of the shear production in the budget equation of the turbulent kinetic energy. Those effects, thus, cannot be captured without a proper model for the process (Yao *et al.*, 2000). This may be the reason why many RANS turbulence model perform poorly in turbulent wake flows. (It is well known that higher order RANS models such as second moment closures predict slower recovery of turbulence properties in the wake region.) Therefore, modelling the pressure-transport effects far away from a wall is an important issue and Yoshizawa (2002) recently discussed the effects of mean strain on the pressure-velocity correlation using the TSDIA. This paper presents another attempt for modelling the mean strain (rapid) part of the pressure-transport term and discussions on its application with a two-component-limit (TCL) second moment closure (SMC) for turbulent wake and separating flows.

MODEL EQUATIONS

The transport equation of the Reynolds stress $\overline{u_iu_j}$ is

$$\frac{D\overline{u_iu_j}}{Dt} = d_{ij} + P_{ij} + \Pi_{ij} - \varepsilon_{ij}, \tag{1}$$

where d_{ij}, P_{ij}, Π_{ij} and ε_{ij} are respectively the diffusion, production, pressure correlation and the dissipation terms of the Reynolds stress. The pressure correlation term is usually split into the pressure-strain ϕ_{ij} and the pressure-transport d^p_{ij} terms:

$$\Pi_{ij} = \phi_{ij} + d^p_{ij}. \tag{2}$$

The first term of the r.h.s. of Eq.(2) has been the "core" term to be modelled and the second term has been regarded to be included in the turbulent diffusion term despite its importance in the recirculating flow region of turbulent wake flows (Yao *et al.*, 2001).

The pressure-transport modelling

The exact pressure correlation term may be written as

$$\begin{aligned}\Pi_{ij} &= -\overline{u_i\frac{\partial p/\rho}{\partial x_j}} - \overline{u_j\frac{\partial p/\rho}{\partial x_i}} \\ &= \underbrace{\overline{\frac{p}{\rho}\left(\frac{\partial u_i}{\partial x_j}+\frac{\partial u_j}{\partial x_i}\right)}}_{\phi_{ij}} + \underbrace{\frac{\partial}{\partial x_m}\left(-\frac{\overline{u_jp}}{\rho}\delta_{im} - \frac{\overline{u_ip}}{\rho}\delta_{jm}\right)}_{d^p_{ij}}\end{aligned} \tag{3}$$

where u_i, p, ρ ,and $\overline{(\ )}$ are the instantaneous velocity, pressure, density, and a Reynolds averaged quantity, respectively. The Poisson equation of the instantaneous pressure and its integration far away from a wall may be written as

$$\frac{1}{\rho}\frac{\partial^2 p}{\partial x_k^2} = -\frac{\partial^2}{\partial x_k\partial x_l}(u_lu_k - \overline{u_lu_k}) - 2\frac{\partial \overline{u_k}}{\partial x_l}\frac{\partial u_l}{\partial x_k} \tag{4}$$

$$\frac{1}{\rho}p = \frac{1}{4\pi}\int_{vol}\left(\frac{\partial^2 u'_ku'_l}{\partial x'_l\partial x'_k} - \frac{\partial^2\overline{u'_ku'_l}}{\partial x'_l\partial x'_k}\right)\frac{dVol}{|\underline{r}|} - \frac{1}{2\pi}\int_{vol}\frac{\partial\overline{u'_k}}{\partial x'_l}\frac{\partial u'_l}{\partial x'_k}\frac{dVol}{|\underline{r}|} \tag{5}$$

Then, the pressure-velocity correlation term may be written as

$$-\frac{\overline{u_jp}}{\rho} = \underbrace{-\frac{1}{4\pi}\int_{vol}\left(\frac{\partial^2\overline{u'_ku'_lu_j}}{\partial r_l\partial r_k}\right)\frac{dVol}{|\underline{r}|}}_{\varphi^p_{j1}} \underbrace{-\frac{1}{2\pi}\frac{\partial\overline{u'_k}}{\partial x'_l}\int_{vol}\frac{\partial\overline{u'_lu_j}}{\partial r_k}\frac{dVol}{|\underline{r}|}}_{\varphi^p_{j2}} \tag{6}$$

Traditionally, the effects of the slow part φ^p_{j1} is considered to be included in the turbulent-transport effects since its linear expression in the third moments results in

$$\varphi^p_{j1} = 0.2\overline{u_ku_ku_j} \tag{7}$$

for satisfying realizability conditions as Lumley (1978) noted. Thus, the slow part is not explicitly considered in this study. The rapid part φ^p_{j2} is presently modelled as a

linear function of both the Reynolds stress and a length-scale vector: ℓ_k , as

$$\varphi^p_{j2} = \frac{\partial \overline{u_k}}{\partial x_l}\gamma^{lj}_k\left(\overline{u_l u_j}, \ell_k\right). \tag{8}$$

There must be several options for determining the length-scale vector. For the third rank tensor γ^{lj}_k , the general form satisfying symmetry in the indexes l, j may be written as

$$\begin{aligned}\frac{\gamma^{lj}_k}{k} &= \beta_1\ell_k\delta_{jl} + \beta_2(\ell_l\delta_{jk} + \ell_j\delta_{kl}) + \beta_3\ell_k a_{jl} \\ &\quad +\beta_4(\ell_l a_{jk} + \ell_j a_{kl}) + \beta_5\ell_m a_{km}\delta_{jl} \\ &\quad +\beta_6\ell_m(a_{lm}\delta_{jk} + a_{jm}\delta_{kl})\end{aligned} \tag{9}$$

where $a_{ij} = \overline{u_i u_j}/k - {}^2/_3\delta_{ij}$,$k = \overline{u_k u_k}/2$ and β 's are the model coefficients. In order to determine the coefficients, the continuity condition:

$$\gamma^{kj}_k = 0 \tag{10}$$

and the two-component-limit (TCL) condition ($d^p_{22} = 0$, if $u_2 = 0$):

$$\frac{\partial}{\partial x_2}\left(\frac{\partial \overline{u_k}}{\partial x_l}\gamma^{l2}_k\right) = 0 \tag{11}$$

are applied. After a moderate amount of algebra, the resultant relation between the coefficients are

$$\beta_2 = -{}^1/_4\beta_1, \beta_3 = {}^3/_2\beta_1, \beta_4 = \beta_5 = 0, \beta_6 = -{}^3/_8\beta_1 \tag{12}$$

and only β_1 is a free coefficient. Thus, the present rapid pressure-transport model may be written as

$$\begin{aligned}d^p_{ij2} &= \frac{\partial}{\partial x_m}\left(\varphi^p_{j2}\delta_{im} + \varphi^p_{i2}\delta_{jm}\right) \\ &= \frac{\partial}{\partial x_m}\left[\frac{\partial \overline{u_k}}{\partial x_l}\beta_1 k\left\{\left(\ell_k\delta_{jl} - \frac{1}{4}(\ell_l\delta_{jk} + \ell_j\delta_{kl}) + \frac{3}{2}\ell_k a_{jl}\right.\right.\right. \\ &\quad \left.\left.\left. -\frac{3}{8}\ell_m(a_{lm}\delta_{jk} + a_{jm}\delta_{kl})\right)\delta_{im} + \left(\ell_k\delta_{il} - \frac{1}{4}(\ell_l\delta_{ik} + \ell_i\delta_{kl})\right.\right.\right. \\ &\quad \left.\left.\left. +\frac{3}{2}\ell_k a_{il} - \frac{3}{8}\ell_m(a_{lm}\delta_{ik} + a_{im}\delta_{kl})\right)\delta_{jm}\right\}\right].\end{aligned} \tag{13}$$

As Lumley (1975) noted, there are several ways of splitting the pressure correlation term Π_{ij} into the pressure-strain and pressure-transport terms. The form discussed by Mansour *et al.*(1988) and used in Craft and Launder (1996) may be written as

$$\Pi_{ij} = \phi^*_{ij} + \underbrace{\frac{\overline{u_i u_j}}{k}\frac{d^p_{kk}}{2}}_{d^{p\,*}_{ij}} \tag{14}$$

where ϕ^*_{ij} and $d^{p\,*}_{ij}$ are the re-defined pressure-strain and pressure-transport terms, respectively. By the model of Eq.(13), d^p_{kk2} vanishes in a fully developed turbulent flow parallel to a wall if ℓ_i vanishes when i is the direction parallel to the wall. Consequently, the pressure-transport term of Eq.(14) does not affect the prediction of such a flow field. Usually, any established RANS model has been calibrated in such flows, and thus the form of Eq.(14) may be a desirable option for implementation into a well calibrated model. Therefore, in the present study, the term:

$$d^{p*}_{ij2} = \frac{\overline{u_i u_j}}{k}\frac{d^p_{kk2}}{2} \tag{15}$$

is simply added to a TCL low Reynolds number (LRN) full second moment closure described in the next subsection.

With the TCL model, the length scale vector ℓ_i in Eq.(13) is presently modelled as

$$\ell_i = \frac{k^{1.5}}{\varepsilon}d^A_i \tag{16}$$

where ε is the dissipation rate of k and d^A_i is Craft and Launder's inhomogeneity indicator defined as

$$d^A_i = \frac{N^A_i}{0.5 + \left(N^A_k N^A_k\right)^{0.5}}, N^A_i = \frac{\partial\left(A^{0.5}k^{1.5}/\varepsilon\right)}{\partial x_i} \tag{17}$$

using the stress flatness parameter (Lumley, 1978) :$A = 1 - (9/8)(a_{ij}a_{ji} - a_{ij}a_{jk}a_{ki})$. The coefficient β_1 in Eq.(13) is currently set as a constant value: -0.05.

The TCL second moment closure

Craft and Launder (1996) proposed a TCL SMC after a series of development for a full realizable SMC by the UMIST group. The employed pressure-strain model is the cubic QI model of Fu (1988). The Craft-Launder model is the first LRN version of its series totally free from topographical parameters. Its redistributive term was modelled as

$$\phi^*_{ij} = \phi_{ij1} + \phi_{ij2} + \phi^{inh}_{ij1} + \phi^{inh}_{ij2}, \tag{18}$$

where $\phi^{inh}_{ij1}, \phi^{inh}_{ij2}$ are the correction terms for inhomogeneity effects. The cubic QI pressure-strain model employs the most general forms for ϕ_{ij1} and ϕ_{ij2} as:

$$\phi_{ij1} = -c_1\tilde{\varepsilon}\left\{a_{ij} + c'_1\left(a_{ik}a_{jk} - \frac{1}{3}A_2\delta_{ij}\right)\right\} - c''_1\tilde{\varepsilon}a_{ij}, \tag{19}$$

$$\begin{aligned}\phi_{ij2} &= -0.6\left(P_{ij} - \frac{1}{3}P_{kk}\delta_{ij}\right) + 0.3a_{ij}P_{kk} \\ &- 0.2\left\{\frac{\overline{u_j u_k}\;\overline{u_i u_l}}{k}S_{kl} - \frac{\overline{u_k u_l}}{k}\left(\overline{u_i u_k}\frac{\partial U_j}{\partial x_l}\right.\right. \\ &\quad \left.\left. +\overline{u_j u_k}\frac{\partial U_i}{\partial x_l}\right)\right\} \\ &- c_2\left\{A_2\left(P_{ij} - D_{ij}\right) + 3a_{mi}a_{nj}\left(P_{mn} - D_{mn}\right)\right\} \\ &+ c'_2\left[\left(\frac{7}{15} - \frac{A_2}{4}\right)\left(P_{ij} - \frac{1}{3}\delta_{ij}P_{kk}\right)\right. \\ &+ 0.1\left\{a_{ij} - \frac{1}{2}\left(a_{ik}a_{kj} - \frac{1}{3}\delta_{ij}A_2\right)\right\}P_{kk} \\ &\quad -0.05a_{ij}a_{kl}P_{kl} \\ &+ 0.1\left\{\left(\frac{\overline{u_i u_m}}{k}P_{jm} + \frac{\overline{u_j u_m}}{k}P_{im}\right)\right. \\ &\quad \left.-\frac{2}{3}\delta_{ij}\frac{\overline{u_l u_m}}{k}P_{lm}\right\} \\ &+ 0.1\left(\frac{\overline{u_i u_l}\;\overline{u_j u_k}}{k^2} - \frac{1}{3}\delta_{ij}\frac{\overline{u_l u_m}\;\overline{u_k u_m}}{k^2}\right) \\ &\quad \times\left(6D_{kl} + 13kS_{kl}\right) \\ &+ \left.0.2\frac{\overline{u_i u_l}\;\overline{u_j u_k}}{k^2}\left(D_{kl} - P_{kl}\right)\right]\end{aligned} \tag{20}$$

where $U_i = \overline{u_i}$,

$$P_{ij} = -\left(\overline{u_i u_k}\frac{\partial U_j}{\partial x_k} + \overline{u_j u_k}\frac{\partial U_i}{\partial x_k}\right),$$

$$D_{ij} = -\left(\overline{u_i u_k}\frac{\partial U_k}{\partial x_j} + \overline{u_j u_k}\frac{\partial U_k}{\partial x_i}\right),$$

$S_{ij} = \partial U_i/\partial x_j + \partial U_j/\partial x_i$, and $A_2 = a_{ij}a_{ij}$.

The inhomogeneity correction terms, $\phi^{inh}_{ij1}, \phi^{inh}_{ij2}$, effectively replaced the traditional wall-reflection terms defining

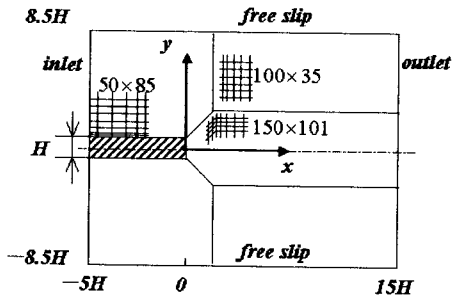

Figure 1: Computational domain and grid for flow behind a rectangular trailing-edge.

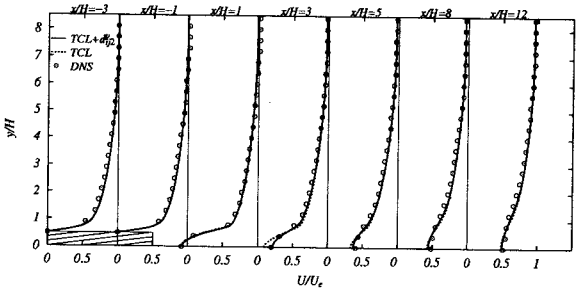

Figure 2: Mean velocity distribution in the wake flow.

inhomogeneity indicators which were basically the gradients of turbulent length scales. This model is realizable and validated in the TCL turbulence boundaries. Even though the model equations are very complicated, it is thought to be rather economical because the realisability contributes to rapid convergence of the solution.

Later, Batten *et al.*(1999) of the UMIST group modified the Craft-Launder model and extended its applicability to compressible flows. The present study thus follows this modified version. Note that although the original Craft-Launder model employs an ASM procedure for the triple moments, Batten *et al.*returned to the usual GGDH model of Daly and Harlow (1970) for the turbulent diffusion process:

$$d_{ij} = \frac{\partial}{\partial x_k}\left\{\left(\nu\delta_{kl} + 0.22\overline{u_k u_l}\frac{k}{\varepsilon}\right)\frac{\partial \overline{u_i u_j}}{\partial x_l}\right\} \qquad (21)$$

where ν is the kinetic viscosity.

The other detailed equations and coefficients of the TCL model are described in Appendix.

RESULTS AND DISCUSSIONS

Rectangular-edge wake flow

Fig.1 illustrates the geometry of the presently considered wake flow behind a rectangular trailing-edge of Yao *et al.*(2001). A developed boundary layer flow comes in from the inlet boundary at the Reynolds number of 1000, based on the free-stream inlet velocity U_e and the trailing edge height H. The present 2D computational grid consists of 5 blocks and 30650 rectangular cells in total. A grid-refinement test with a finer grid having twice node points in each direction has indicated that numerical errors are unimportant with the present grid (see Fig.3). Numerical computations have

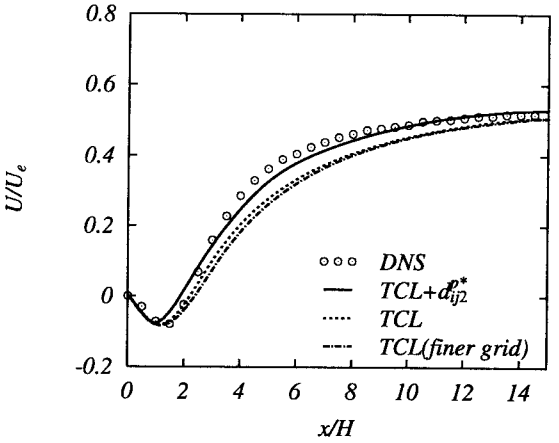

Figure 3: Streamwise velocity along the centerline.

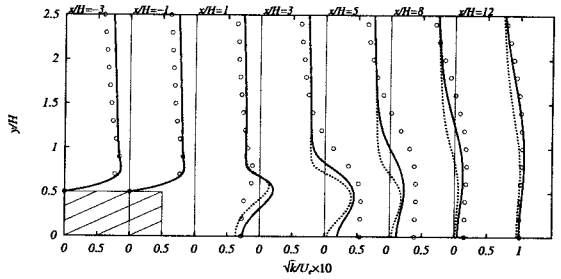

Figure 4: Turbulence energy distribution in the wake flow; o o o:DNS, ——:TCL+d^{p*}_{ij2}, ·····:TCL.

been performed by a general unstructured grid code of Suga *et al.*(2001) using the third order scheme for the convection terms.

Fig.2 compares the mean velocity distribution with that of the DNS of Yao *et al.*(2001). Although both of the TCL models with and without d^{p*}_{ij2} term perform equally well, discrepancies can be seen on the centerline $y/H = 0$. (The TCL model means the TCL model without d^{p*}_{ij2} hereafter.) To confirm this, Fig.3 compares the predicted streamwise mean velocity along the centerline behind the trailing-edge. It is obvious that including the d^{p*}_{ij2} term reasonably improves recovery in the wake region though it leads to a little shorter recirculation.

Fig.4 compares the turbulence energy distribution. Although the agreement is not perfect, the d^{p*}_{ij2} term generally improves the predictive performance of the TCL model. In the distribution of the Reynolds stresses (Fig.5(a)-(d)), there can be also found clear discrepancies between the models. In the recirculation region at $x/H = 1$, the TCL model overpredicts the shear stress $-\overline{uv}$ (Fig.5(a)) resulting in a little high level of streamwise normal stress $\overline{u^2}$ (Fig.5(b)). Although including the d^{p*}_{ij2} term tends to enhance the overprediction of the shear stress there, it does not affect the $\overline{u^2}$ and does improve the $\overline{v^2}$ distribution near the centerline (Fig.5.(c)). In the sections downstream of the recirculation ($x/H \geq 3$), all the profiles of the development of the Reynolds stresses are obviously improved by the d^{p*}_{ij2} term though $\overline{v^2}$ is still rather smaller near the centerline. This encourages the present modelling strategy though further considerations may be needed for the recirculating region.

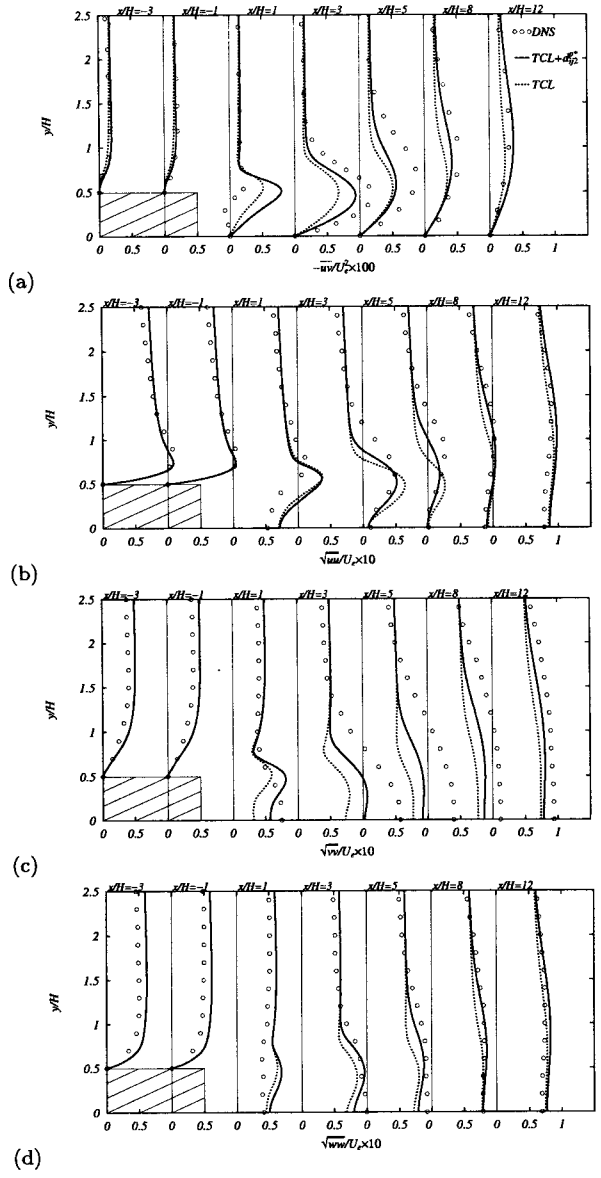

Figure 5: Reynolds stress distribution in the wake flow.

Fig.6 shows the budget distribution of the turbulence energy equation by the TCL model with d^{p*}_{ij2} in the recirculating region at $x/H = 1$. Clearly no predicted process accords well with the DNS data. (The dissipation ε and the turbulent diffusion d^t_k need to be improved. Due to the overprediction of $-\overline{uv}$, the production P_k is overpredicted though P_k itself does not need any modelling.) As shown in Fig.7, according to the decrease of the mean strain towards the centerline ($y/H = 0$), the predicted distribution of d^p_k decreases rapidly from $y/H = 0.6$. However, the DNS indicates that although its second peak is around $y/H = 0.6$, its peak appears around $y/H = 0.4$. Since the turbulent diffusion process, which is a triple moment, is not significant in the region shown in Fig.7, the DNS suggests that the slow pressure-transport should not significant there also. Thus, owing to the profiles of the mean strain shown in Fig.7, some functional magnitude needs to be multiplied to the rapid pressure-transport model for reproducing the peak profile. Or, a higher order form of the third rank tensor model may need to be considered.

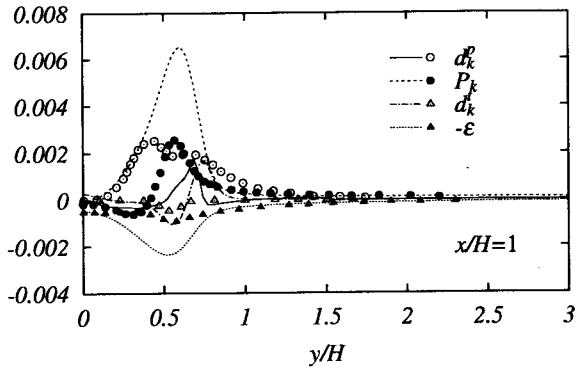

Figure 6: Budget of the k equation in the recirculating region of the wake flow; symbols: DNS, lines:TCL+d^{p*}_{ij2}.

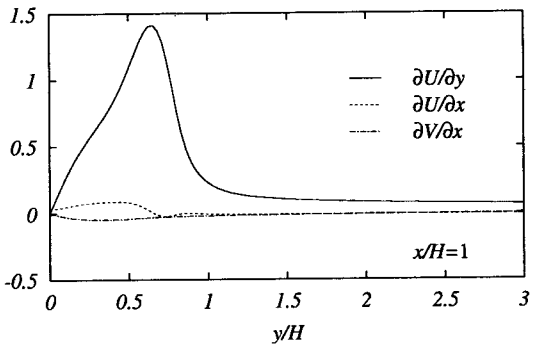

Figure 7: Mean velocity gradient in the recirculating region of the wake flow.

Back-step flow

Another evaluation of the effects of the d^{p*}_{ij2} term has been performed in the back-step flow of Kasagi and Matsunaga (1995). Its Reynolds number is 5500 based on the step height H and the centerline velocity U_c. The computational grid used has a structure similar to that for the trailing-edge wake flow and consists of 19000 rectangular cells in the domain of $-5H \leq x \leq 30H$. The grid resolution is comparable to that of wake flow and has been confirmed to be enough since a finer grid with twice node points in each direction has produced less than 2% longer reattachment length than that by the present grid. (The predicted reattachment length is 6.3 for both the cases with and without the d^{p*}_{ij2} term though the experimentally measured one is 6.5.)

Fig.8(a) shows the distribution of the mean velocity. It is obvious that the d^{p*}_{ij2} term does not affect the mean velocity distribution and both the model predictions are well agree with the experiments. In the distribution of the Reynolds shear and normal stresses (Fig.8(b)(c)), although there can bee seen slight discrepancies between the predictions, both the model predictions agree well with the experiments. This implies that almost no significant effect of the d^{p*}_{ij2} term can be found in this flow field.

Fig.9 shows the distribution of the processes of the turbulence energy equation by the TCL model with the d^{p*}_{ij2} in the recirculating region at $x/H = 2$. The relative magnitude of the pressure-transport d^p_k is smaller than that in the wake flow (Fig.6). This is the reason of its ineffectiveness on

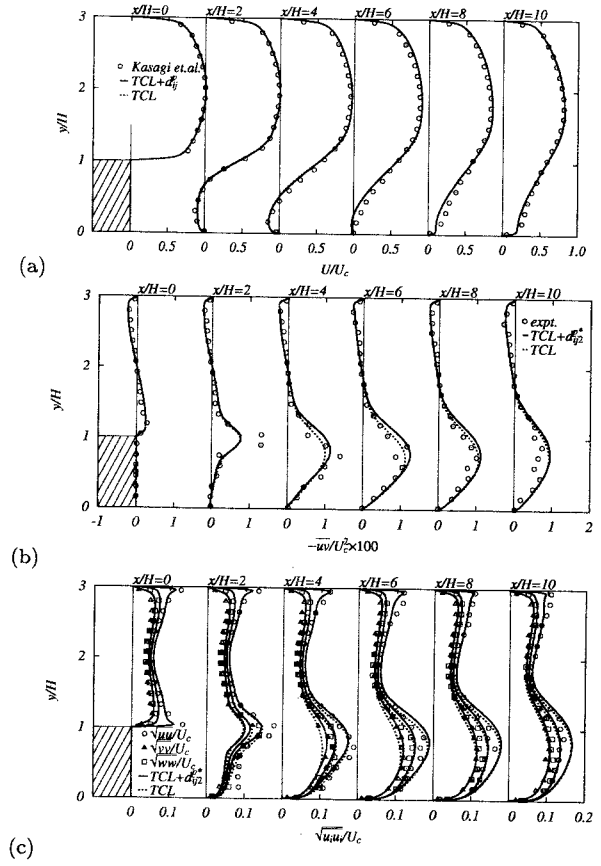

Figure 8: Mean velocity and Reynolds stress distribution in the back-step flow.

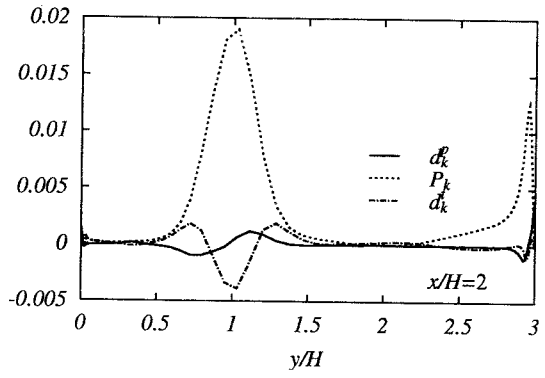

Figure 9: Processes of the k equation in the recirculating region of the back-step flow; lines:TCL+d_{ij2}^{p*}.

the predictions shown in Fig.8. Le *et al.*(1997) also showed very small relative magnitude of d_k^p in the recirculating region of their low-Reynolds number back-step flow by DNS. $y/H = 0.4$

CONCLUDING REMARKS

In the present study, the rapid part of the pressure-transport process of the Reynolds stress equation is modelled using the two-component-limit condition. The effects of the proposed term in the two-component-limit second moment closure are discussed through the application to a turbulent wake flow behind a rectangular trailing-edge and a turbulent back step flow. The following remarks are concluded:

1. The rapid pressure-transport model is effective to improve generally the prediction of the turbulent wake flow. However, further consideration for its functional coefficient or higher order form is needed to obtain more reasonable results.

2. The effects of the rapid pressure-transport model tends to be marginal in the low-Reynolds number back step flow. This complies with the DNS of the similar back step flow and implies that the general tendency of the process is reasonably captured by the present model.

APPENDIX: ADDITIONAL MODEL EQUATIONS OF THE TCL SMC

The model equations which are not described in the main part are summarised below.

To compensate the near wall variation of the pressure transport, the additional term:

$$-\frac{1}{\rho}\frac{\partial}{\partial x_k}\left[-\rho c_{pd}(0.5d_k + 1.1d_k^A)(\nu\varepsilon k A A_2)^{1/2}\right] \qquad (22)$$

is added to Eq.(14), where d_i is another inhomogeneity indicator:

$$d_i = \frac{N_i}{0.5 + (N_k N_k)^{\frac{1}{2}}}, \quad N_i = \frac{\partial(k^{1.5}/\varepsilon)}{\partial x_i}, \qquad (23)$$

and the coefficient is

$$c_{pd} = 1.5(1 - A^2)[\{1 + 2\exp(-R_t/40)\}A_2 + 0.4R_t^{-1/4}\exp(-R_t/40)].$$

The inhomogeneity correction terms:

$$\begin{aligned}\phi_{ij1}^{inh} &= f_{w1}\frac{\varepsilon}{k}\left(\overline{u_l u_k}d_l^A d_k^A\delta_{ij} - \frac{3}{2}\overline{u_i u_k}d_j^A d_k^A - \frac{3}{2}\overline{u_j u_k}d_i^A d_k^A\right)\\ &\quad + f_{w2}\frac{\varepsilon}{k^2}\left(\overline{u_m u_n}\ \overline{u_m u_l}d_n^A d_l^A\delta_{ij} - \frac{3}{2}\overline{u_i u_m}\ \overline{u_m u_l}d_j^A d_l^A\right.\\ &\quad \left. - \frac{3}{2}\overline{u_j u_m}\ \overline{u_m u_l}d_i^A d_l^A\right) \qquad (24)\\ \phi_{ij2}^{inh} &= f_I k\frac{\partial U_l}{\partial x_n}d_l d_n\left(d_i d_j - \frac{1}{3}d_k d_k\delta_{ij}\right) \qquad (25)\end{aligned}$$

are used.

The dissipation tensor is modelled as

$$\varepsilon_{ij} = (1 - f_\varepsilon)(\varepsilon'_{ij} + \varepsilon''_{ij})/D + \frac{2}{3}\delta_{ij}f_\varepsilon\varepsilon, \qquad (26)$$

with

$$\begin{aligned}\varepsilon'_{ij} &= 2\nu\frac{\partial\sqrt{k}}{\partial x_m}\left(\frac{\partial\sqrt{k}}{\partial x_i}\frac{\overline{u_j u_m}}{k} + \frac{\partial\sqrt{k}}{\partial x_j}\frac{\overline{u_i u_m}}{k}\right)\\ &\quad + 2\nu\frac{\partial\sqrt{k}}{\partial x_k}\frac{\partial\sqrt{k}}{\partial x_m}\frac{\overline{u_k u_m}}{k}\delta_{ij} + \frac{\overline{u_i u_j}}{k}\varepsilon, \qquad (27)\\ \varepsilon''_{ij} &= f_R\varepsilon\left(2\frac{\overline{u_l u_k}}{k}d_l^A d_k^A\delta_{ij} - \frac{\overline{u_i u_l}}{k}d_l^A d_j^A - \frac{\overline{u_j u_l}}{k}d_l^A d_i^A\right) \qquad (28)\end{aligned}$$

where $D = (\varepsilon'_{kk} + \varepsilon''_{kk})/(2\varepsilon)$ and

$$\begin{aligned}f_\varepsilon &= 20A^{1.5}(A \le 0.05)\\ &= \sqrt{A}(A > 0.05). \qquad (29)\end{aligned}$$

The transport equation for the isotropic dissipation rate $\tilde{\varepsilon}$ ($\equiv \varepsilon - 2\nu(\partial\sqrt{k}/\partial x_k)(\partial\sqrt{k}/\partial x_k)$) is modelled as

Table 1: Model coefficients and functions in the TCL second moment closure.

$c_1 = 3.2 f_A \sqrt{A_2} f_{Rt}$	$c_2 = \min[0.55\{1-\exp(\frac{-A^{3/2}R_t}{100})\}, \frac{3.24}{1+S}]$	$c_1' = 1.1$	$c_2' = \min(0.6, \sqrt{A}) + f_S$
$f_{w1} = 3(1-\sqrt{A}) f_{R_t}'$	$f_{w2} = 0.6 A_2 (1-\sqrt{A}) f_{R_t}'' + 0.1$	$c_1'' = A^{1/2}$	$f_{R_t} = \min\{\left(\frac{R_t}{200}\right)^2, 1\}$
$f_A = \sqrt{A/14}$, $A \le 0.05$	$f_{R_t}' = \min\left\{1, \max\left(0, 1-\frac{R_t-55}{70}\right)\right\}$	$f_I = 3 f_A$	$f_{R_t}'' = \min\left\{1, \max\left(0, 1-\frac{R_t-50}{200}\right)\right\}$
$= A/\sqrt{0.7}$, $0.05 < A < 0.7$	$f_R = (1-A)\min\{(R_t/80)^2, 1\}$		$f_\varepsilon = 20 A^{3/2}$, $A \le 0.05$
$= \sqrt{A}$, $A \ge 0.7$	$f_S = \frac{3.5(S-\Omega)}{3+S+\Omega} - 4\sqrt{6}\min(S_I, 0)$		$= \sqrt{A}$, $A > 0.05$

$$\frac{D\tilde{\varepsilon}}{Dt} = \frac{\partial}{\partial x_k}\left\{\left(\nu\delta_{kl} + 0.18\overline{u_k u_l}\frac{k}{\varepsilon}\right)\frac{\partial \tilde{\varepsilon}}{\partial x_l}\right\} + c_{\varepsilon 1}\frac{P_{kk}}{2}\frac{\tilde{\varepsilon}}{k} - c_{\varepsilon 2}\frac{\tilde{\varepsilon}^2}{k} - \frac{(\varepsilon-\tilde{\varepsilon})\tilde{\varepsilon}}{k} + P_{\varepsilon 3} + Y_E \quad (30)$$

where $c_{\varepsilon 1} = 1.44, c_{\varepsilon 2} = 1.92$, and

$$P_{\varepsilon 3} = 0.4\nu\overline{u_i u_j}\frac{k}{\varepsilon}\frac{\partial^2 U_k}{\partial x_i \partial x_l}\frac{\partial^2 U_k}{\partial x_j \partial x_l}. \quad (31)$$

The length-scale correction term of Iacovides and Raisee (1999):

$$Y_E = 0.83\frac{\tilde{\varepsilon}^2}{k}\max\{F(F+1)^2, 0\} \quad (32)$$

is employed with

$$F = \frac{1}{c_l}\left(\frac{\partial(k^{1.5}/\varepsilon)}{\partial x_j}\frac{\partial(k^{1.5}/\varepsilon)}{\partial x_j}\right)^{1/2} - \{1-\exp(-B_\varepsilon R_t) + B_\varepsilon R_t \exp(-B_\varepsilon R_t)\}, \quad (33)$$

$c_l = 2.55$ and $B_\varepsilon = 0.1069$.

All the other model coefficients and functions are listed in Table 1.

REFERENCES

Batten, P., Craft, T.J., Leschziner, M.A., and Loyau, H., 1999, "Reynolds-stress-transport modeling for compressible aerodynamics applications," *AIAA J.*, Vol.37, pp.785–797.

Craft, T.J., and Launder, B.E., 1996, "A Reynolds-stress closure designed for complex geometries", *Int. J. Heat Fluid Fl.*, Vol.17, pp.245–254.

Daly, B.J., and Harlow, F.H., 1970, "Transport equation in turbulence" *Phys. Fluids* Vol.13, pp2634–2649.

Fu, S., 1988, "Computational modelling of turbulent swirling flows with second-moment closures," PhD Thesis, UMIST, Manchester.

Iacovides, H., Raisee, M.,1999, "Recent progress in the computation of flow and heat transfer in internal cooling passages of turbine blades," *Int. J. Heat Fluid Fl.*, Vol.20, pp.320–328

Kasagi, N., and Matsunaga, A., 1995, "Three-dimensional particle-tracking velocimetry measurement of turbulence statistics and energy budget in a backward-facing step flow," *Int. J. Heat Fluid Fl.*, Vol.16, pp.477–485.

Kawamura, H., and Kawashima, N.,1994 "A proposal of $k-\tilde{\varepsilon}$ model with relevance to the near-wall turbulence," *Proc. Int. Symp. on Turbulence, Heat and Mass Transfer*, Lisbon, Vol.2, P.I.1.1–P.I.1.4.

Le, H., Moin, P., and Kim, J., 1997, "Direct numerical simulation of turbulent flow over a backward-facing step," *J. Fluid Mech.*, Vol. 330, pp.349–374.

Lumley, J.L., 1978, "Computational modeling of turbulent flows," *Adv. in Applied Mech.*, Vol.18, pp.123–176.

Lumley, J.L., 1975, "Pressure strain correlation," *Phys. Fluids*, Vol.19, p.750.

Mansour, N.N., Kim, J. and Moin,P., 1988, "Reynolds-stress and dissipation-rate budgets in a turbulent channel flow," *J. Fluid Mech.*, Vol. 194, pp.15–44.

Nagano, Y., and Shimada, M., 1995, "Rigorous modeling of dissipation-rate equation using direct simulations," *JSME Int. J. B*,Vol.38, pp.51–59.

Spalart, P.R., 1988, "Direct simulation of a turbulent boundary layer up to $R_\theta = 1410$," *J. Fluid Mech.*, Vol.187, pp.61–98.

Suga, K., Nagaoka, M., Horinouchi, N., Abe, K., and Kondo, K., 2001, "Application of a three equation cubic eddy viscosity model to 3-D turbulent flows by the unstructured grid methods," *Int. J. Heat Fluid Fl.*, Vol.22, pp.259–271.

Yao, Y.F., Savill, A.M., Sandham, N.D., and Dawes, W.N., 2000, "Simulation of turbulent trailing-edge flow using unsteady RANS and DNS ," *Proc. the 3rd Int. Symp. on Turbulence, Heat and Mass Transfer*, Nagoya, Japan, pp.463–470.

Yao, Y.F., Thomas, T.G., Sandham, N.D., and Williams,J.J.R., 2001, "Direct numerical simulation of turbulent flow over a rectangular trailing edge," *Theore. Comput. Fluid Dynamics*, Vol.14, pp.337–358.

Yoshizawa, A., 1987, "Statistical modeling of a transport equation for the kinetic energy dissipation rate," *Phys. Fluids*, Vol. 30, pp.628–631.

Yoshizawa, A, 2002, "Statistical analysis of mean-flow effects on the pressure-velocity correlation," *Phys. Fluids*, Vol. 14, pp.1736–1744.